Inverse Problems, Design and Optimization Symposium
Rio de Janeiro, Brazil, 2004

TOPOLOGICAL-SHAPE SENSITIVITY METHOD APPLIED TO INVERSE POISSON'S CONDUCTIVITY PROBLEM

A.A. Novotny, T. Guinzani F., R.A. Feijóo, E. Taroco
Laboratório Nacional de Computação Científica LNCC/MCT,
Av. Getúlio Vargas 333, 25651-075 Petrópolis - RJ, Brasil
novotny@lncc.br, feij@lncc.br, etam@lncc.br

C. Padra
Centro Atómico Bariloche,
8400 Bariloche, Argentina
padra@cab.cnea.gov.ar

ABSTRACT

The Topological Derivative concept has been widely accepted as a powerful framework to obtain the optimal topology for several engineering problems. This derivative furnishes the sensitivity of the problem when the domain under consideration is perturbed by the introduction of a hole. In the present paper, we apply the novel Topological-Shape Sensitivity Method as a systematic methodology for computing the Topological Derivative in Inverse Poisson's Conductivity Problem. In particular, we extend the Topological Derivative concept to compute the sensitivity of a cost function when a small circular incrustation is introduced at any point of the bulk material. The preceding approach leads to a new method to solve inverse conductivity problem. Finally, we present numerical experiments in steady-state heat conduction problem, showing that the developed methodology allow us to identify the shape and topology of unknown incrustations.

INTRODUCTION

The Topological Derivative leads to a scalar function that supplies, for each point of the domain under consideration, the sensitivity of a given cost function when a small hole is created [3, 5, 10, 14, 19]. More recently, in [8, 9, 17] a new method to compute the Topological Derivative via Shape Sensitivity Analysis was proposed. This method, called Topological-Shape Sensitivity Method has two main features. First, leads to a simpler and more general procedure to compute the Topological Derivative than others found in the current literature. Second, allow us to consider several kind of cost functions and any type of boundary conditions on the hole.

It has been already accepted that Topological Derivative furnishes a powerful tool for Topological Optimization [4]. Nevertheless, this concept is wider. In fact, it also could be applied to inverse problems (see, for instance, [7, 20]) and to simulate physical phenomena with changes on their configuration.

Alternatively, the same theory developed for Topological Derivative can be used to calculate the sensitivity of a given cost function when, instead of a hole, a small incrustation is introduced at a point in the domain. This concept called Configurational Derivative [16] can be naturally applied in the inverse problems context [13]. In particular, on identification of defects in mechanical components and properties characterization in heterogeneous media among others [1].

To show the applicability of the Configurational Derivative to inverse problems, we have limited ourself to the steady-state heat conduction problem on rigid solids. The adopted cost function is a quadratic form of the difference between a measured (observed) and a calculated temperature. This sensitivity leads up to a new method to solve inverse problems, in our particular case the Inverse Poisson's Conductivity Problem. Finally, we present numerical experiments showing that the developed methodology allow us to identify unknown incrustations by means of temperature measurements in the domain.

CONFIGURATIONAL DERIVATIVE

The same theory developed to calculate the Topological Derivative via Shape Sensitivity Analysis can be used to compute the sensitivity of a given cost function when a small incrustation is introduced at a point in the domain, as shown in fig. (1). This sensitivity leads to a scalar function called Configurational Derivative.

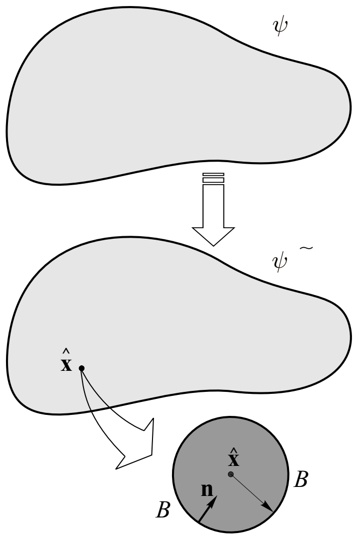

Figure 1: Configurational Derivative Concept

Let us consider an open bounded domain $\Omega \subset \mathbb{R}^2$ with a smooth boundary Γ. If the domain Ω is perturbed by introducing a small incrustation at an arbitrary point $\hat{\mathbf{x}} \in \Omega$, we have a new domain $\tilde{\Omega}_\epsilon = \Omega_\epsilon \cup B_\epsilon$, where $\overline{B}_\epsilon = B_\epsilon \cup \partial B_\epsilon$ is a ball of radius ϵ centered at the point $\hat{\mathbf{x}} \in \Omega$, $\Omega_\epsilon = \Omega - B_\epsilon$ and $\Gamma_\epsilon = \Gamma \cup \partial B_\epsilon$. In another words, Ω_ϵ denotes the bulk material, B_ϵ the incrustation and their union represents the domain under consideration $\tilde{\Omega}_\epsilon$ (see fig. 1).

Thus, we have the original domain without incrustation Ω and the new one $\tilde{\Omega}_\epsilon = \Omega_\epsilon \cup B_\epsilon$ with a small incrustation B_ϵ. Considering a cost function ψ, the Configurational Derivative is defined as

$$D_C(\hat{\mathbf{x}}) := \lim_{\epsilon \to 0} \frac{\psi(\tilde{\Omega}_\epsilon) - \psi(\Omega)}{f(\epsilon)} , \qquad (1)$$

where $f(\epsilon)$ is a negative function that decreases monotonically so that $f(\epsilon) \to 0$ with $\epsilon \to 0^+$.

In [17] the authors proposed a new method, called Topological-Shape Sensitivity Method, which allow us to use the whole mathematical framework (and results) developed for the Shape Sensitivity Analysis (see [2, 11, 12, 15, 18, 21, 22, 23] and references therein) to compute the Topological Derivative. Likewise, we can apply this methodology to compute the Configurational Derivative (eq. 1). The main result obtained in [17] is given by the following Theorem (for more detail of the Topological-Shape Sensitivity Method and its applications see [16]):

Theorem 1 *Let $f(\epsilon)$ be a function chosen in order to $0 < |D_C(\hat{\mathbf{x}})| < \infty$, then the Configurational Derivative given by eq. (1) can be written as*

$$D_C(\hat{\mathbf{x}}) = \lim_{\epsilon \to 0} \frac{1}{f'(\epsilon)} \frac{d}{d\tau} \psi(\tilde{\Omega}_\tau) \bigg|_{\tau=0} , \qquad (2)$$

where $\tau \in \mathbb{R}$ is used to parameterize the domain. That is, for τ small enough, we have

$$\tilde{\Omega}_\tau := \left\{ \mathbf{x}_\tau \in \mathbb{R}^2 : \mathbf{x}_\tau = \mathbf{x} + \tau \mathbf{v},\ \mathbf{x} \in \tilde{\Omega}_\epsilon, \tau \in \mathbb{R}^+ \right\} ,$$

with $\tilde{\Omega}_\tau = \Omega_\tau \cup B_{\epsilon_\tau}$, $\epsilon_\tau = \epsilon + \tau$ and $\tilde{\Omega}_\tau|_{\tau=0} = \tilde{\Omega}_\epsilon$, being $\mathbf{v}$ the shape change velocity *defined by*

$$\begin{cases} \mathbf{v} = -\mathbf{n} & on\ \partial B_\epsilon \\ \mathbf{v} = \mathbf{0} & on\ \Gamma \end{cases} . \qquad (3)$$

In addition,

$$\frac{d}{d\tau} \psi(\tilde{\Omega}_\tau) \bigg|_{\tau=0} = \lim_{\tau \to 0} \frac{\psi(\tilde{\Omega}_\tau) - \psi(\tilde{\Omega}_\epsilon)}{\tau} \qquad (4)$$

is the shape sensitivity of the cost function in relation to the domain perturbation characterized by $\mathbf{v}$.

Proof. The reader interested in the proof of this result may refer to [8, 17] ■

This Theorem points out that the Configurational Derivative may be obtained through the Shape Sensitivity Analysis of the cost function (Topological-Shape Sensitivity Method). Therefore, results from Shape Sensitivity Analysis can be used to calculate the Configurational Derivative in a simple and constructive way considering eq. (2).

INVERSE POISSON'S CONDUCTIVITY PROBLEM

In this section, the Configurational Derivative is computed in steady-state heat conduction problem on rigid solids, taking as cost function a quadratic form of the difference between a measured (observed) and a calculated temperature.

Statement of the Problem

Let us consider a rigid solid represented by $\tilde{\Omega}_\epsilon = \Omega_\epsilon \cup B_\epsilon \subset \mathbb{R}^2$, with a small incrustation B_ϵ centered at $\hat{\mathbf{x}} \in \tilde{\Omega}_\epsilon$, submitted to an excitation b in the domain $\tilde{\Omega}_\epsilon$. Considering continuity of the solution u_ϵ on ∂B_ϵ, the variational formulation of the problem can be written as follows: find $u_\epsilon \in \mathcal{U}_\epsilon$, such that

$$a_\epsilon\left(u_\epsilon,\eta\right) = l_\epsilon\left(\eta\right) \quad \forall \eta \in \mathcal{V}_\epsilon \ , \tag{5}$$

where the bilinear form $a_\epsilon(u_\epsilon, \eta)$ and the linear functional $l_\epsilon(\eta)$ are written, in this particular case, as

$$a_\epsilon\left(u_\epsilon,\eta\right) := \int_{\Omega_\epsilon} k^e \nabla u_\epsilon \cdot \nabla \eta + \int_{B_\epsilon} k^i \nabla u_\epsilon \cdot \nabla \eta \ , \tag{6}$$

$$l_\epsilon\left(\eta\right) := \int_{\tilde{\Omega}_\epsilon} b\eta - \int_{\Gamma_N} \bar{q}\eta \ . \tag{7}$$

where $\mathcal{U}_\epsilon$ the admissible functions set and $\mathcal{V}_\epsilon$ the admissible variations space, that are defined by

$$\mathcal{U}_\epsilon = \{u_\epsilon \in H^1(\tilde{\Omega}_\epsilon) : u_\epsilon|_{\Gamma_D} = \overline{u}\} \tag{8}$$

$$\mathcal{V}_\epsilon = \{\eta \in H^1(\tilde{\Omega}_\epsilon) : \eta|_{\Gamma_D} = 0\} \ , \tag{9}$$

where Γ_D and Γ_N are the Dirichlet and Neumann boundaries such that $\Gamma = \Gamma_D \cup \Gamma_N$, with $\Gamma_D \cap \Gamma_N = \emptyset$; $\bar{u}$ and $\bar{q}$ are the temperature and heat flux prescribed on Γ_D and Γ_N; k^e and k^i respectively are the thermal conductivity coefficients of bulk material (represented by Ω_ϵ) and incrustation (represented by B_ϵ).

Finally, the cost function is defined as a quadratic form of the difference between a measured (observed) and a calculated temperature, that is

$$\mathcal{J}_\epsilon(u_\epsilon) := \psi(\tilde{\Omega}_\epsilon) = \int_{\tilde{\Omega}_\epsilon} (u_\epsilon - u^*)^2 \ , \tag{10}$$

where u^* is a temperature measurement and u_ϵ is the solution of the variational problem given by eq. (5).

Since the state equation must be verified in all perturbed configuration $\tilde{\Omega}_\tau$, the corresponding solution u_τ satisfies the following variational problem: find $u_\tau \in \mathcal{U}_\tau$, such that

$$a_\tau\left(u_\tau,\eta\right) = l_\tau\left(\eta\right) \quad \forall \eta \in \mathcal{V}_\tau \ , \ \forall \tau \geq 0 \ , \tag{11}$$

where $\mathcal{U}_\tau$ is the admissible functions set and $\mathcal{V}_\tau$ is the admissible variations space, both defined on the perturbed domain $\tilde{\Omega}_\tau$. In addition, $a_\tau\left(u_\tau,\eta\right)$ and $l_\tau\left(\eta\right)$ are given by

$$a_\tau\left(u_\tau,\eta\right) := \int_{\Omega_\tau} k^e \nabla_\tau u_\tau \cdot \nabla_\tau \eta + \int_{B_{\epsilon_\tau}} k^i \nabla_\tau u_\tau \cdot \nabla_\tau \eta \ , \tag{12}$$

$$l_\tau\left(\eta\right) := \int_{\tilde{\Omega}_\tau} b\eta - \int_{\Gamma_N} \bar{q}\eta \ . \tag{13}$$

Likewise, the cost function written in the perturbed configuration $\tilde{\Omega}_\tau$ becomes

$$\mathcal{J}_\tau(u_\tau) := \psi(\tilde{\Omega}_\tau) = \int_{\tilde{\Omega}_\tau} (u_\tau - u^*)^2 \ , \tag{14}$$

where u_τ is the solution of eq. (11).

Configurational Derivative Calculation

The shape derivative of the cost function eq. (4), taking the state equation as the constraint, can be formally written as

$$\left\{ \begin{array}{l} \dfrac{d}{d\tau} \mathcal{J}_\tau(u_\tau)|_{\tau=0} \\ a_\tau\left(u_\tau, \eta\right) = l_\tau(\eta) \quad \forall \eta \in \mathcal{V}_\tau \end{array} \right. . \tag{15}$$

This problem can be solved using the Lagrangian method that consists in relaxing the constraint of the problem by Lagrangian multipliers. Therefore, the Lagrangian defined in the perturbed configuration $\tilde{\Omega}_\tau$

$$\mathcal{L}_\tau\left(u_\tau, \lambda_\tau\right) = \mathcal{J}_\tau\left(u_\tau\right) + a_\tau\left(u_\tau, \lambda_\tau\right) - l_\tau\left(\lambda_\tau\right) \ , \tag{16}$$

allow us to compute the shape derivative of the cost function as follows

$$\frac{d}{d\tau}\mathcal{J}_\tau\left(u_\tau\right) = \frac{\partial}{\partial\tau}\mathcal{L}_\tau\left(u_\tau, \lambda_\tau\right) \ , \tag{17}$$

where $u_\tau \in \mathcal{U}_\tau$ is the solution of the state equation (eq. 11) and $\lambda_\tau \in \mathcal{V}_\tau$ is the Lagrangian multiplier, solution of the *adjoint equation* given by

$$a_\tau(\lambda_\tau, \eta) = -\left\langle \frac{\partial}{\partial u_\tau} \mathcal{J}_\tau(u_\tau), \eta \right\rangle \ \forall \eta \in \mathcal{V}_\tau \ . \tag{18}$$

In this particular case, the adjoint equation becomes: find $\lambda_\tau \in \mathcal{V}_\tau$, such that

$$a_\tau(\lambda_\tau, \eta) = -2 \int_{\tilde{\Omega}_\tau} (u_\tau - u^*)\eta \ \ \forall \eta \in \mathcal{V}_\tau \ . \tag{19}$$

From the Reynolds' transport theorem and considering the Lagrangian method, the derivative of the cost function, at $\tau = 0$, becomes

$$\left. \frac{d}{d\tau} \mathcal{J}_\tau(u_\tau) \right|_{\tau=0} = \int_{\tilde{\Omega}_\epsilon} \mathbf{\Sigma}_\epsilon \cdot \nabla \mathbf{v} \ , \tag{20}$$

where $\mathbf{\Sigma}_\epsilon$ can be seen as an extension of the Eshelby's energy-momentum tensor (see for instance [6, 22]). It is important to mention that the energy momentum tensor was first introduced by Eshelby into elastostatics of three dimensional bodies in the context of infinitesimal deformations. This tensor also plays a central role in the same author's development of continuum approach when studying defects in solid media. Furthermore, $\mathbf{\Sigma}_\epsilon$ can be decomposed as

$$\mathbf{\Sigma}_\epsilon|_{\Omega_\epsilon} := \mathbf{\Sigma}_\epsilon^e \quad \text{and} \quad \mathbf{\Sigma}_\epsilon|_{B_\epsilon} := \mathbf{\Sigma}_\epsilon^i \ . \tag{21}$$

where $\mathbf{\Sigma}_\epsilon^e$ and $\mathbf{\Sigma}_\epsilon^i$ are respectively given by

$$\begin{aligned} \mathbf{\Sigma}_\epsilon^e &= \left[(u_\epsilon - u^*)^2 + k^e \nabla u_\epsilon \cdot \nabla \lambda_\epsilon - b\lambda_\epsilon\right] \mathbf{I} \\ &- k^e (\nabla u_\epsilon \otimes \nabla \lambda_\epsilon + \nabla \lambda_\epsilon \otimes \nabla u_\epsilon) \ , \qquad (22) \\ \mathbf{\Sigma}_\epsilon^i &= \left[(u_\epsilon - u^*)^2 + k^i \nabla u_\epsilon \cdot \nabla \lambda_\epsilon - b\lambda_\epsilon\right] \mathbf{I} \\ &- k^i (\nabla u_\epsilon \otimes \nabla \lambda_\epsilon + \nabla \lambda_\epsilon \otimes \nabla u_\epsilon) \ . \qquad (23) \end{aligned}$$

Moreover, it is well known that shape derivative only depends on the value of $\mathbf{v}$ at the boundary. In fact, it is straightforward to verify that

$$\int_{\tilde{\Omega}_\epsilon} \operatorname{div} \mathbf{\Sigma}_\epsilon \cdot \mathbf{v} = 0 \quad \forall \mathbf{v} \ \Leftrightarrow \ \operatorname{div} \mathbf{\Sigma}_\epsilon = \mathbf{0} \ . \tag{24}$$

Therefore, from divergence theorem and considering eq. (24), eq. (20) yields

$$\left. \frac{d}{d\tau} \mathcal{J}_\tau(u_\tau) \right|_{\tau=0} = \int_{\Gamma_\epsilon} \left(\mathbf{\Sigma}_\epsilon^e - \mathbf{\Sigma}_\epsilon^i\right) \mathbf{n} \cdot \mathbf{v} \ , \tag{25}$$

remembering that $\tilde{\Omega}_\epsilon = \Omega_\epsilon \cup B_\epsilon$ and that $\mathbf{n}$ is the outward unit normal vector defined on Γ_ϵ.

Recalling the definition of the velocity field given by eq. (3), the shape derivative of the cost function reduces to an integral along the boundary ∂B_ϵ, that is

$$\left. \frac{d}{d\tau} \mathcal{J}_\tau(u_\tau) \right|_{\tau=0} = -\int_{\partial B_\epsilon} \left(\mathbf{\Sigma}_\epsilon^e - \mathbf{\Sigma}_\epsilon^i\right) \mathbf{n} \cdot \mathbf{n} \ , \tag{26}$$

where

$$\begin{aligned} \mathbf{\Sigma}_\epsilon^e \mathbf{n} \cdot \mathbf{n} &= (u_\epsilon^e - u^*)^2 - b\lambda_\epsilon^e \\ &+ k^e \frac{\partial u_\epsilon^e}{\partial t} \frac{\partial \lambda_\epsilon^e}{\partial t} - k^e \frac{\partial u_\epsilon^e}{\partial n} \frac{\partial \lambda_\epsilon^e}{\partial n} \ , \qquad (27) \\ \mathbf{\Sigma}_\epsilon^i \mathbf{n} \cdot \mathbf{n} &= (u_\epsilon^i - u^*)^2 - b\lambda_\epsilon^i \\ &+ k^i \frac{\partial u_\epsilon^i}{\partial t} \frac{\partial \lambda_\epsilon^i}{\partial t} - k^i \frac{\partial u_\epsilon^i}{\partial n} \frac{\partial \lambda_\epsilon^i}{\partial n} \ . \qquad (28) \end{aligned}$$

Using the continuity condition of the solutions u_ϵ and λ_ϵ on the boundary of the incrustation ∂B_ϵ, we have

$$\left\{ \begin{array}{l} \dfrac{\partial u_\epsilon^e}{\partial t} = \dfrac{\partial u_\epsilon^i}{\partial t} \\ \dfrac{\partial \lambda_\epsilon^e}{\partial t} = \dfrac{\partial \lambda_\epsilon^i}{\partial t} \end{array} \right. , \quad \left\{ \begin{array}{l} \dfrac{\partial u_\epsilon^e}{\partial n} = \dfrac{k^i}{k^e} \dfrac{\partial u_\epsilon^i}{\partial n} \\ \dfrac{\partial \lambda_\epsilon^e}{\partial n} = \dfrac{k^i}{k^e} \dfrac{\partial \lambda_\epsilon^i}{\partial n} \end{array} \right. . \tag{29}$$

Upon considering the above results in eq. (26) and further substitution in Theorem 1 (eq. 2), the Configurational Derivative becomes

$$\begin{aligned} D_C(\hat{\mathbf{x}}) &= -\lim_{\epsilon \to 0} \frac{1}{f'(\epsilon)} \int_{\partial B_\epsilon} \left(k^e - k^i\right) \\ & \left(\frac{\partial u_\epsilon^i}{\partial t} \frac{\partial \lambda_\epsilon^i}{\partial t} + \frac{k^i}{k^e} \frac{\partial u_\epsilon^i}{\partial n} \frac{\partial \lambda_\epsilon^i}{\partial n} \right) \ . \qquad (30) \end{aligned}$$

In order to obtain the final expression of the Configurational Derivative, we need to explicitly know the behaviour of the solutions u_ϵ and λ_ϵ when $\epsilon \to 0$, as well as their normal and tangential derivatives. Thus, an asymptotic analysis of u_ϵ and λ_ϵ shall be performed. Therefore, from this analysis (see [16]), it is possible to compute the limit with $\epsilon \to 0$ in eq. (30) to obtain

$$D_C(\hat{\mathbf{x}}) = 2k^e \left(\frac{k^e - k^i}{k^e + k^i} \right) \nabla u \cdot \nabla \lambda \ , \tag{31}$$

where $f(\epsilon) = -\text{meas}(B_\epsilon)$ and u and λ are the solutions of the state and adjoint equations, respectively, both defined in the original domain

Ω (without incrustation). From an analysis of eq. (31) we observe that it is sufficient to compute the solutions associated to the original problem (without incrustation), that is u and λ, to obtain the sensitivity of the cost function when an incrustation is created in an arbitrary point $\hat{\mathbf{x}} \in \Omega$. Thus, the Configurational Derivative can be obtained without additional cost, besides that necessary in the calculation of ∇u and $\nabla \lambda$.

Configurational Derivative for several measurements

If we have several temperature measurements, the cost function can be defined as a sum of a quadratic form of the difference between observed and calculated temperatures for each measurement, that is

$$\mathcal{J}(u) := \sum_{n=1}^{M} \int_{\Omega} (u_n - u_n^*)^2 \; , \qquad (32)$$

being u_n^* the n-th temperature measurement and M the number of measurements. In this case, the Configurational Derivative becomes

$$D_C(\hat{\mathbf{x}}) = 2k^e \left(\frac{k^e - k^i}{k^e + k^i} \right) \sum_{n=1}^{M} \nabla u_n \cdot \nabla \lambda_n \; , \quad (33)$$

where u_n and λ_n respectively are the solutions of state and adjoint equations defined in the original domain Ω for the n-th measurement.

NUMERICAL RESULTS

The solutions u and λ, defined in the original domain Ω (without incrustation), are computed through the Finite Element Method.

Normally, measurement u^* is obtained from experiments in laboratory. However, on the following examples, u^* is also calculated through the Finite Element Method. Therefore, function u^* represents the solution of the state equation defined on the domain including the incrustations that shall be identified.

From analysis of eq. (1), the unknown incrustations that we want to identify must be positioned where the cost function is **more** sensible, that is, where $D_C(\hat{\mathbf{x}})$ attains large absolute values.

It should be mention that thermal conductivity coefficient of the incrustation k^i is **unknown**. On the other hand, we assume that thermal conductivity coefficient of the bulk material k^e is **known**.

We assume, for all examples shown in this paper, the excitation $b = 0$.

Example 1

The present example shows the behaviour of the Configurational Derivative when the properties of an incrustation are modified. More specifically, we want to study what happens to $D_C(\hat{\mathbf{x}})$ when the thermal conductivity coefficient of the incrustation k^i assumes different values. In addition, we assume that the thermal conductivity coefficient k^e of the bulk material remains fixed.

The domain of this problem consists in a square $\Omega = (0, 2.0) \times (0, 2.0)$, where on the bottom we have $\overline{u} = 0$ and on the top $\overline{q} = 1.0$.

To obtain the observed temperature u^*, two cases are analyzed both with a centered circular incrustation with radius $R = 0.2$ and $k^e = 1.0$. Case A has $k^i_A = 0.1$ and Case B has $k^i_B = 10.0$. The target domain can be seen in fig. (2).

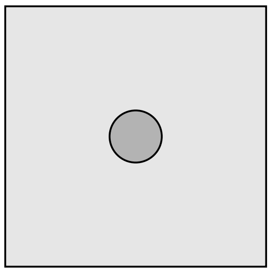

Figure 2: Example 1 - Target domain.

The scalar field $\nabla u \cdot \nabla \lambda$, which is proportional to $D_C(\hat{\mathbf{x}})$ (eq. 31), obtained for Case A and Case B are shown in figs. (3, 4), respectively. The incrustation is clearly identified by the maximum absolute values of $D_C(\hat{\mathbf{x}})$ (see isolines on the mentioned figures).

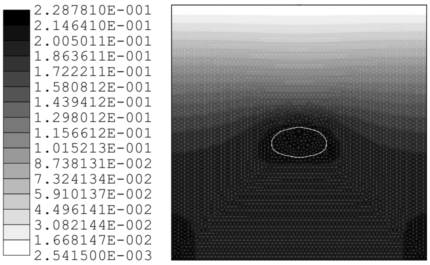

Figure 3: Example 1 - Field $\nabla u \cdot \nabla \lambda$ for Case A: $k^i_A = 0.1$. The isoline value is 2.2×10^{-1}.

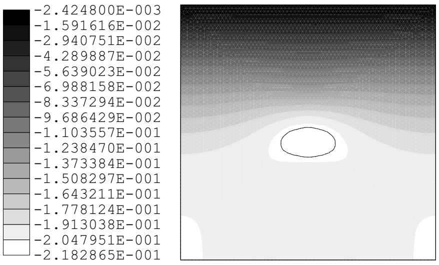

Figure 4: Example 1 - Field $\nabla u \cdot \nabla \lambda$ for Case B: $k^i_B = 10$. The isoline value is -2.1×10^{-1}.

We can also observe that $D_C(\hat{\mathbf{x}})$ keeps stable even for large differences of properties between incrustation and bulk material, as seen in figs. (3, 4), where the thermal conductivity coefficients of the incrustation are 10 times smaller and bigger, respectively, than the thermal conductivity coefficient of the bulk material.

Comparing figs. (3, 4) the field $\nabla u \cdot \nabla \lambda$ in Case B has a negative sign, while in Case A it has a positive sign. Since $D_C(\hat{\mathbf{x}})$ must be positive (we want to minimize the cost function), we can also infer from its definition (eq. 1):

- if $\nabla u \cdot \nabla \lambda > 0$, then $k^i < k^e$;
- if $\nabla u \cdot \nabla \lambda < 0$, then $k^i > k^e$.

It should be notice that the k^i value is not known *a priori*.

Example 2

This example shows the behaviour of the Configurational Derivative when we have several temperature measurements (see eq. 33).

The domain of this problem is the same of the previous one (see fig. 2). Four distinct measurements, $M = 4$, are analyzed modifying the boundaries where we prescribe $\overline{u}_n = 0$ and $\overline{q}_n = 1.0$. The first one, $n = 1$, is obtained choosing $\overline{u}_1$ on the bottom and $\overline{q}_1$ on the top. On the second measurement, $n = 2$, we have $\overline{u}_2$ on the right and $\overline{q}_2$ on the left. The third measurement, $n = 3$, is obtained choosing $\overline{u}_3$ on the top and $\overline{q}_3$ on the bottom. Finally, on the fourth one, $n = 4$, are prescribed $\overline{u}_4$ on the left and $\overline{q}_4$ on the right of the square. The thermal conductivity coefficient of the bulk material is $k^e = 1.0$.

The above procedure is also used to compute the observed temperature u^*_n, for $n = 1, 2, 3, 4$, in the target domain shown in fig. (2), where the thermal conductivity coefficient of the incrustation is $k^i = 0.8$.

The sum of fields $\nabla u_n \cdot \nabla \lambda_n$ obtained in each measurement, which is proportional to $D_C(\hat{\mathbf{x}})$ given by eq. (33), can be seen in fig. (5), where the incrustation is once again clearly identified by the maximum values of $D_C(\hat{\mathbf{x}})$ (see isoline on the mentioned figure).

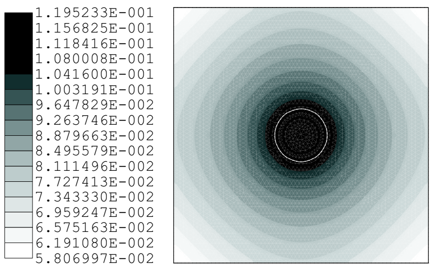

Figure 5: Example 2 - Sum of fields $\nabla u_n \cdot \nabla \lambda_n$ obtained in each measurement. The isoline value is 1.1×10^{-1}.

Example 3

The present example, like the previous one, shows the behaviour of the Configurational Derivative when we have several temperature measurements (see eq. 33). Nevertheless, in this example the target domain has several incrustations with the same thermal conductivity coefficient k^i.

The domain of this problem consists in a rectangle $\Omega = (0, 2.0) \times (0, 1.5)$. Once again, four distinct measurements are analyzed changing the sides of the rectangle where we prescribe $\overline{u}_n = 0$ and $\overline{q}_n = 1.0$; the first measurement is obtained choosing $\overline{u}_1$ on the bottom and $\overline{q}_1$ on the top; on the second one, we have $\overline{u}_2$ on the right and $\overline{q}_2$ on the left; the third measurement is obtained choosing $\overline{u}_3$ on the top and $\overline{q}_3$ on the bottom; and on the last one are prescribed $\overline{u}_4$ on the left and $\overline{q}_4$ on the right of the square. The thermal conductivity coefficient of the bulk material is $k^e = 1.0$.

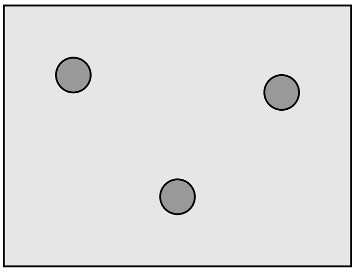

Figure 6: Example 3 - Target domain.

The same measurements above are performed to compute u^*, obtaining four different temperature measurements in a domain that has three circular incrustations whose thermal conductivity coefficient is $k^i = 0.8$. The target domain is shown in fig. (6). In fig. (7) it is shown the sum of fields $\nabla u_n \cdot \nabla \lambda_n$ obtained in each measurement, where the incrustations are clearly identified by the maximum values of $D_C(\hat{\mathbf{x}})$ (see isoline on the mentioned figure).

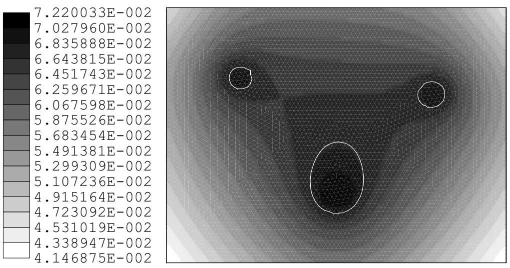

Figure 7: Example 3 - Sum of fields $\nabla u_n \cdot \nabla \lambda_n$ obtained in each measurement. The isoline value is 6.8×10^{-2}.

CONCLUSION

The main goal of this work is to show the applicability of the Configurational Derivative (eq. 1) in problems where the shape and topology of incrustations must be characterized. From eq. (1) the Configurational Derivative $D_C(\hat{\mathbf{x}})$ is such that

$$\psi(\tilde{\Omega}_\epsilon) = \psi(\Omega) + f(\epsilon) D_C(\hat{\mathbf{x}}) + O(f(\epsilon)) \quad (34)$$

where

$$\lim_{\epsilon \to 0} \frac{O(f(\epsilon))}{f(\epsilon)} = 0 \, . \quad (35)$$

Therefore $D_C(\hat{\mathbf{x}})$ can be seen as a first order correction to $\psi(\Omega)$ to obtain $\psi(\tilde{\Omega}_\epsilon)$. This last interpretation of the Configurational Derivative can be used to devise an alternative reconstruction method: since the solution of the inverse problem is given by the domain $\tilde{\Omega}_\epsilon$ which minimizes the functional $\psi(\tilde{\Omega}_\epsilon)$, we can choose the points in Ω (which does not contain any incrustation) where the value of the Configurational Derivative attains its highest absolute values. Note that these points give the largest decrease in the cost functional when incrustations are placed on them.

In particular, considering the steady-state heat conduction problem, we have shown that the Configurational Derivative allows to identify the shape and topology of the unknown incrustations. Moreover, its thermal conductivity coefficient is also characterized by the sign of the Configurational Derivative. On the other hand, classical approach for this kind of problem based on shape optimization has an intrinsic limitation: the number of incrustation in the bulk material must be known *a priori*. In order to overcome this difficulty the Congurational Derivative evolves as an interesting alternative. In fact, the unknown field is identified even when there are several incrustations. This issue is also discussed in [7].

Finally, we would like to say that the Configurational Derivative can also be utilized as a new approach for mechanical modelling of problems such that cavitation, plasticity, ductile fracture, phase change, damage among others.

ACKNOWLEDGEMENTS

This research was partly supported by the projects FINEP/CNPq-PRONEX, CT-PETRO/CNPq, PCI-LNCC/MCT, FAPERJ (E-26/150.712/2003) and by CONICET (Argentina). The support from these agencies is greatly appreciated.

References

[1] H.D. Bui. *Inverse Problems in the Mechanics of Materials: an Introduction.* CRC Press, 1994.

[2] J. Céa. Problems of Shape Optimal Design. In Haug & Céa [12].

[3] J. Céa, S. Garreau, Ph. Guillaume & M. Masmoudi. The Shape and Topological Optimizations Connection. *Comput. Methods Appl. Mech. Engrg.*, **188**:713-726, 2000.

[4] H.A. Eschenauer & N. Olhoff. Topology Optimization of Continuum Structures: A Review. *Appl. Mech. Review*, **54**:331-390, 2001.

[5] H.A. Eschenauer, V.V. Kobelev & A. Schumacher. Bubble Method for Topology and Shape Optimization of Structures. *Struct. Optim.*, **8**:42-51, 1994.

[6] J.D. Eshelby. The Elastic Energy-Momentum Tensor. *Journal of Elasticity*, **5**:321-335, 1975.

[7] G. R. Feijóo. An Imaging Method in Diffraction Tomography Based on the Topological Derivative. To appear on IEEE Symposium, 2004.

[8] R.A. Feijóo, A.A. Novotny, C. Padra & E. Taroco. The Topological Derivative for the Poisson's Problem. *Math. Models Methods Appl. Sciences*, **13-12**:1-20, 2003.

[9] R.A. Feijóo, A.A. Novotny, C. Padra & E. Taroco. The Topological-Shape Sensitivity Method and its Application in 2D Elasticity. To appear on *J. Comput. Methods Sciences Engrg.*, 2003.

[10] S. Garreau, Ph. Guillaume & M. Masmoudi. The Topological Asymptotic for PDE Systems: The Elasticity Case. *SIAM J. Control Optim.*, **39**:1756-1778, 2001.

[11] E.J. Haug, K.K. Choi & V. Komkov. *Design Sensitivity Analysis of Structural Systems.* Academic Press, 1986.

[12] E.J. Haug & J. Céa. Proceedings: *Optimization of Distributed Parameters Structures*, Iowa, EUA, 1981.

[13] V. Isakov. *Inverse Problems for Partial Differential Equations.* Springer, 1998.

[14] T. Lewiński & J. Sokolowski. Energy change due to the appearance of cavities in elastic solids. *Int. J. Solids Struct.*, **40**:1765-1803, 2003.

[15] F. Murat & J. Simon. *Sur le Contrôle par un Domaine Géométrique.* Doctoral Thesis, Université Pierre et Marie Curie, Paris VI, France, 1976.

[16] A.A. Novotny. *Análise de Sensibilidade Topológica.* Doctoral Thesis, LNCC-MCT, Petrópolis, Brasil, 2003 (http://www.lncc.br/∼novotny/principal.htm).

[17] A.A. Novotny, R.A. Feijóo, C. Padra & E. Taroco. Topological Sensitivity Analysis. *Comput. Methods Appl. Mech. Engrg.*, **192**:803-829, 2003.

[18] O. Pironneau. *Optimal Shape Design for Elliptic Systems.* Springer-Verlag, 1984.

[19] J. Sokolowski & A. Żochowski. On the Topological Derivative in Shape Optimization. *SIAM J. Control Optim.*, **37**:1251-1272, 1999.

[20] J. Sokolowski & A. Żochowski. Topological Derivatives for Elliptic Problems. *Inverse Problems*, **15**:123-134, 1999.

[21] J. Sokolowski & J.-P. Zolésio. *Introduction to Shape Optimization - Shape Sensitivity Analysis.* Springer-Verlag, 1992.

[22] E. Taroco. G.C. Buscaglia & R.A. Feijóo. Second-Order Shape Sensitivity Analysis for Nonlinear Problems. *Struct. Optim.*, **15**:101-113, 1998.

[23] J.-P. Zolézio. The Material Derivative (or Speed) Method for Shape Optimization. In Haug & Céa [12].